



# Perylene diimide based ‘turn-on’ fluorescence sensor for detection of Pd<sup>2+</sup> in mixed aqueous media

Hai-xia Wang <sup>a,b,\*</sup>, Yue-he Lang <sup>a</sup>, Hui-xuan Wang <sup>a</sup>, Jing-jing Lou <sup>a</sup>, Hai-ming Guo <sup>a,b</sup>, Xi-you Li <sup>c,\*</sup>

<sup>a</sup> School of Chemistry and Chemical Engineering, Key Laboratory of Green Chemical Media and Reactions of Ministry of Education, Henan Normal University, Xinxiang 453007, China

<sup>b</sup> School of Environmental Science, Henan Normal University, Xinxiang 453007, China

<sup>c</sup> School of Chemistry and Chemical Engineering, Shandong University, Jinan 250100, China

## ARTICLE INFO

### Article history:

Received 12 November 2013

Received in revised form 21 January 2014

Accepted 27 January 2014

Available online 31 January 2014

### Keywords:

Perylene tetracarboxylic diimide

Fluorescence sensor

PDI-1

Pd<sup>2+</sup>

Turn-on

## ABSTRACT

A perylene diimide (PDI) based fluorescence chemosensor (**PDI-1**) for Pd<sup>2+</sup> was prepared. **PDI-1** showed a remarkable fluorescence enhancement (over 120-fold) in the presence of Pd<sup>2+</sup> in mixed aqueous media with high selectivity and sensitivity. Moreover, the dramatically ‘off–on’ fluorescence response concomitantly induced the obvious color change from dark purple to brilliant pink, which could also be identified by naked eyes easily. The low limit for Pd<sup>2+</sup> detection was found to be as small as 10<sup>-9</sup> mol/L. Hence, **PDI-1** is a highly promising fluorescent chemosensor for the direct determination of residual Pd<sup>2+</sup> in chemical medicines and environment samples.

© 2014 Elsevier Ltd. All rights reserved.

## 1. Introduction

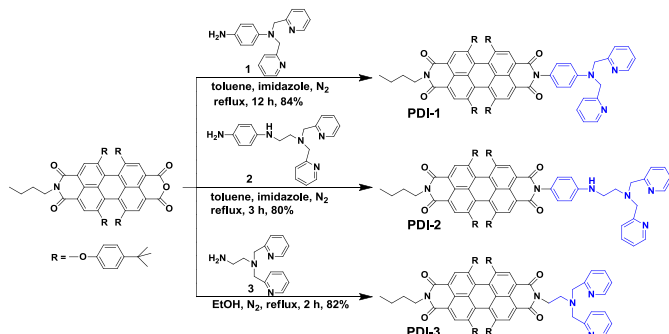
In recent years, fluorescent chemosensors for sensing and monitoring heavy and transitional metal ions (HTM) are an attractive field due to their high sensitivity and simplicity.<sup>1</sup> Among the metal ions, palladium as a rare transition metal of platinum group metals, is widely used as catalysts in the synthesis of various drugs and chemical products.<sup>2</sup> However, palladium can accumulate in vivo, bind to proteins, and other biomacromolecules leading to degradation of DNA and disturbance of a variety of cellular processes.<sup>3</sup> The proposed maximum dietary intake of Pd is <15 µg/day<sup>-1</sup> per person and its threshold in drugs is 5–10 ppm.<sup>3,4</sup> Thus, it is necessary to develop highly selective and sensitive fluorescent chemosensors for the quick detection of palladium species in the living system and natural environment. Among the literature reports, most of fluorescent sensors displayed high selectivity for palladium by adopting two kinds of signaling mechanisms, including rhodamine spirolactam-ring-opening-based process and palladium catalyzed nonrhodamine-based chemical reaction, such as the deprotection of propargyl ethers.<sup>5,6</sup> However, photo-induced

electron transfer (PET), as a well-known design strategy for various fluorescence chemosensors for metal ions,<sup>7</sup> was scarcely employed in the development of fluorescence sensors for palladium. In this regard, we are interested in construction of a new PET-based ‘turn-on’ fluorescence chemosensors for Pd<sup>2+</sup>.

Perylene tetracarboxylic diimide derivatives widely used as fluorophore with good electron accepting ability<sup>8</sup> have generated great interest in the field of photonic materials because of their excellent light and thermal stabilities, high fluorescence efficiency, and good semiconducting properties.<sup>9</sup> Hence, PDIs are also favorable fluorophores for fluorescence sensors towards HTMs.<sup>7q,10</sup> For example, Shangguan and co-workers have reported a PDI-based turn-on fluorescent sensor for Zn<sup>2+</sup> and Cd<sup>2+</sup> ions by adjusting the pH of media (acetonitrile–HEPES buffer, 1/1, v/v).<sup>7q</sup> He and co-workers have developed a fluorometric and colorimetric sensor for Cu<sup>2+</sup> by grafting PDI onto the surface of gold nanoparticles.<sup>10a</sup> Additionally, two ‘off–on’ PDI-based fluorescence probes for paramagnetic species Ni<sup>2+</sup> and Fe<sup>3+</sup> in DMF were reported in our previous works.<sup>10b</sup>

Herein, three PDIs derivatives **PDI-1**, **PDI-2**, and **PDI-3** were rationally designed and synthesized for the purpose of sensing HTMs (Scheme 1). The PDI with four substituents at the bay positions was chosen as fluorophore and di(2-pyridylmethyl)amine (DPA) group was used as receptor owing to their powerful chelating

\* Corresponding authors. E-mail addresses: hxwang5270@163.com (H.-xia Wang), xyyouli@sdu.edu.cn (X.-you Li).



**Scheme 1.** Molecular structures and synthesis of **PDI-1**, **PDI-2**, and **PDI-3**.

ability to many transitional metal ions.<sup>7q,10b,11</sup> The different linker, including aromatic benzyl ring, *N*-ethyl-aniline, and saturated ethyl groups, connected the fluorophores with DPA moieties, respectively. Apparently, the expected photoinduced receptor-to-fluorophore electron transfer (PET) can occur when DPA units are not involved in metal ion binding, they can act as electron donors, which quenches the fluorescence of the PDI while the fluorophores are excited. Once the DPA units coordinated with metal ions, the PET process between DPA and PDI would be inhibited and thus the strong fluorescence of PDI fluorophore would be restored.

The results revealed that **PDI-1** showed excellent selectivity and sensitivity for Pd<sup>2+</sup> ions over other competing metal ions in mixed aqueous media (DMF/H<sub>2</sub>O, v/v, 7:1). The remarkable fluorescence increase over 120-fold was triggered upon addition of Pd<sup>2+</sup>, and the low detect limit was determined to be  $7.32 \times 10^{-9}$  M, which was sufficiently low to detect the nanomolar concentration of Pd<sup>2+</sup>. **PDI-1** was shown to be a promising fluorescent chemosensor for the direct quantitative determination of residual palladium (0–15 ppm) in chemicals and natural environment.

## 2. Results and discussion

### 2.1. Synthesis

The detailed synthetic procedures of these three PDI derivatives were described in **Scheme 1**. *N*-n-Butyl-1,6,7,12-tetra(4-tert-butyl-phenoxy)perylene-3,4:9,10-tetracarboxylic-3,4-anhydride-9,10-imide were condensed with compound **1** and compound **2**, respectively, in toluene with imidazole as the base to give rise to **PDI-1** in 84% yield and **PDI-2** in 80% yield. **PDI-3** was synthesized by refluxing *N*-n-butyl-1,6,7,12-tetra(4-tert-butyl-phenoxy)perylene-3,4:9,10-tetracarboxylic-3,4-anhydride-9,10-imide and compound **3** in absolute ethanol to give an 82% yield. The new compounds, **PDI-1**, **PDI-2**, and **PDI-3** were fully characterized by <sup>1</sup>H and <sup>13</sup>C NMR, and HR-ESI spectra.

### 2.2. Absorption and fluorescence spectra of PDI-1, PDI-2, and PDI-3

The absorption spectra of these three compounds in dichloromethane (DCM) showed a strong band centered around 580 nm, which was typical for PDIs with four substituents at the bay positions.<sup>12</sup> These results suggest that the connection of DPA groups at the imide nitrogens through different bridges does not affect the ground state of PDI. This is reasonable because the frontier molecular orbital knots at the imide nitrogens block the interactions between the DPA and PDI units.<sup>9b,13</sup> Due to the same reason, the UV-vis absorption spectra of **PDI-1** showed almost negligible changes in the presence of metal ions in their solution. However, the fluorescence spectra of **PDI-1**, **PDI-2**, and **PDI-3** in DCM were

significantly different as shown in **Fig. 1**. The parameters about absorption and emission spectra of **PDI-1**, **PDI-2**, and **PDI-3** derivatives in different solvents at room temperature were summarized in **Table S1**. As expected, the fluorescence from the PDI fluorophore in **PDI-1** ( $\Phi_F=0.01$ , using *N,N*-bis(normal-butyl-1,7-bis-(*tert*-butylphenoxy)perylene-3,4:9,10-tetracarboxylic-diimide) in DCM solution as reference compound,<sup>10b</sup>  $\Phi_F=1$ ) was completely quenched due to the quick and efficient PET process from nitrogen lone pair of DPA to PDI fluorophore. Similar fluorescence quenching was also observed for **PDI-2** ( $\Phi_F=0.09$ ). But the fluorescence quantum yield of **PDI-3** ( $\Phi_F=0.5$ ) is relative large, which indicates that the PET process in this compound is less efficient and slow.

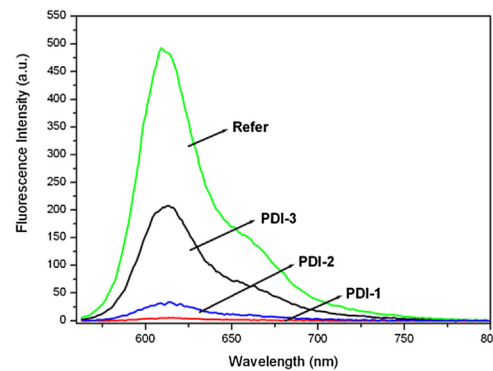


**Fig. 1.** Fluorescence spectra of **PDI-1**, **PDI-2**, and **PDI-3** in DCM solutions at room temperature (*N,N*-Bis(normal-butyl-1,7-bis-(*tert*-butylphenoxy)perylene-3,4:9,10-tetracarboxylic-diimide) in DCM solution as reference compound,<sup>10b</sup>  $\Phi_F=1$ ),  $\lambda_{ex}=540$  nm,  $[PDI-1]=10$   $\mu$ M,  $[PDI-2]=10$   $\mu$ M,  $[PDI-3]=10$   $\mu$ M, [Refer]=10  $\mu$ M,  $\lambda_{ex}=540$  nm, Slit: 2.5 nm, 2.5 nm.

### 2.3. Recognition to different metal ions

The recognition behaviors of PDIs toward different metal ions (8.0 equiv) were investigated by fluorescence and UV-vis spectra. As shown in **Fig. 2**, in the absence of various metal ions, **PDI-1** showed no fluorescence in DMF/H<sub>2</sub>O (7/1, v/v) solution ( $\Phi_F=0.0041$ ) due to the highly efficient PET process between DPA moiety and PDI fluorophore. In the presence of Ni<sup>2+</sup>, Hg<sup>2+</sup>, Co<sup>2+</sup>, Zn<sup>2+</sup>, and Cd<sup>2+</sup>, very small increase on the intensity of fluorescence of **PDI-1** was observed. In the presence of other metal ions, including Cr<sup>3+</sup>, Mn<sup>2+</sup>, Fe<sup>3+</sup>, Cu<sup>2+</sup>, Ag<sup>+</sup>, and Pb<sup>2+</sup>, under identical experimental conditions, the fluorescence intensity changes were negligible. However, when Pd<sup>2+</sup> was added, a significant emission peak centered at around 620 nm appeared immediately. The

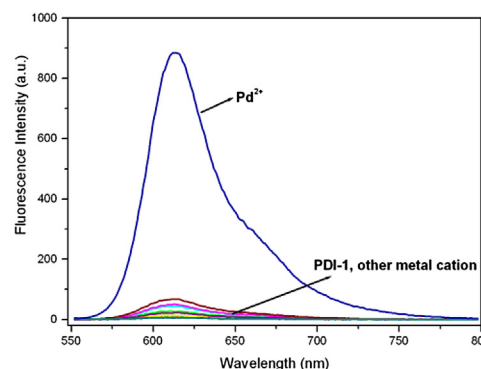


**Fig. 2.** Fluorescence spectra change of **PDI-1** (6.0  $\mu$ M) upon addition of different metal ions (8.0 equiv) including Cr<sup>3+</sup>, Mn<sup>2+</sup>, Fe<sup>3+</sup>, Co<sup>2+</sup>, Ni<sup>2+</sup>, Cu<sup>2+</sup>, Zn<sup>2+</sup>, Ag<sup>+</sup>, Cd<sup>2+</sup>, Hg<sup>2+</sup>, Pb<sup>2+</sup>, and Pd<sup>2+</sup> in DMF/H<sub>2</sub>O (v/v, 7/1),  $\lambda_{ex}=540$  nm, Slit: 2.5 nm; 5.0 nm.

enhancement factors (EFs) of the fluorescence of **PDI-1** in the presence of various metal ions (8.0 equiv) were shown in Fig. 3. In the presence of  $\text{Pd}^{2+}$  ions, the fluorescence intensity of **PDI-1** increased by over 120-fold ( $\Phi_F=0.52$ ). The EFs of  $\text{Ni}^{2+}$ ,  $\text{Hg}^{2+}$ ,  $\text{Co}^{2+}$ ,  $\text{Zn}^{2+}$ , and  $\text{Cd}^{2+}$  were 10, 7, 6, 3, and 2, respectively. **PDI-1** thus exhibits obvious ‘turn-on’ fluorescence response, and displays a remarkably high selectivity towards  $\text{Pd}^{2+}$  in mixed aqueous media. But for **PDI-2** and **PDI-3**, no distinct fluorescence response could be observed upon the addition of various metal ions including  $\text{Pd}^{2+}$  in mixed aqueous solutions (Fig. S7). The experimental results indicated clearly that **PDI-2** and **PDI-3** had no response and selectivity for metal ions in  $\text{DMF}/\text{H}_2\text{O}$  (7/1, v/v) solutions.

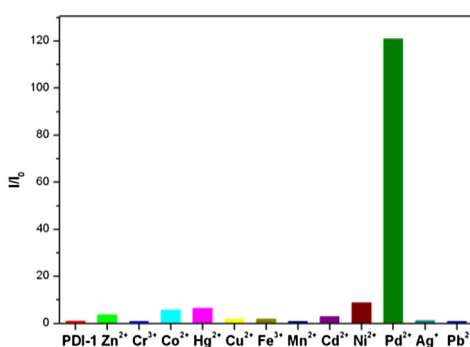


**Fig. 3.** Fluorescence responses of **PDI-1** (6.0  $\mu\text{M}$ ) to various metal cations in  $\text{DMF}/\text{H}_2\text{O}$  (v/v, 7/1),  $\lambda_{\text{ex}}=540$  nm, Slit: 2.5 nm; 5.0 nm.

The high selectivity of **PDI-1** for  $\text{Pd}^{2+}$  is surprising because the DPA moiety as cation chelating groups usually displayed high selectivity towards  $\text{Zn}^{2+}$ ,  $\text{Cu}^{2+}$ ,  $\text{Cd}^{2+}$  or  $\text{Ni}^{2+}$  as reported in previous literature.<sup>10b,11</sup> For fluorescence probes, as we know, the varied binding properties of DPA to metal ions are dependent on the fluorophore, linker, and experimental conditions, such as solvents. The dramatic fluorescence increase of **PDI-1** in the presence of  $\text{Pd}^{2+}$  could be related to the expected PET process in it. When the nitrogen atom connecting directly to the phenyl linker in DPA unit coordinated to the selected metal ions, the PET process was hindered and the fluorescence of the fluorophore restored. Additionally, the reported crystal structure of the complex obtained from DPA ligand and  $\text{Pd}^{2+}$  revealed clearly the coordination of the aniline N with the palladium (II).<sup>14</sup>

Although **PDI-1** exhibited highly remarkable ‘turn-on’ fluorescence upon addition of  $\text{Pd}^{2+}$  in mixed aqueous solutions, the absorption spectra of **PDI-1** and **PDI-1** with different metal ions including  $\text{Pd}^{2+}$  showed no obvious changes as mentioned above (Fig. S8). These results thus suggested that addition of  $\text{Pd}^{2+}$  ions induced no detectable aggregating behavior. It was worth noting that due to the remarkable restored fluorescence, the solution of **PDI-1** with  $\text{Pd}^{2+}$  ions displayed obvious color change from dark purple to brilliant pink (inset of Fig. S8), which could be identified by naked eyes. Consequently, **PDI-1** provides a visual method to discriminate  $\text{Pd}^{2+}$  ions from other transitional metal ions.

#### 2.4. Fluorescence titration and competition experiments

A fluorescence titration experiment of **PDI-1** (5.0  $\mu\text{M}$ ) with  $\text{Pd}^{2+}$  ions was conducted in  $\text{DMF}/\text{H}_2\text{O}$  (7/1, v/v) at 25 °C (Fig. 4). Upon gradual addition of  $\text{Pd}^{2+}$  to the solutions of **PDI-1** (up to 10 equiv), the fluorescence at around 620 nm was enhanced progressively. A brilliant orange color of **PDI-1** was clearly observed under UV lamp (inset of Fig. 4), indicating that **PDI-1** could be a promising selective fluorescent chemosensor for the direct detection of residual

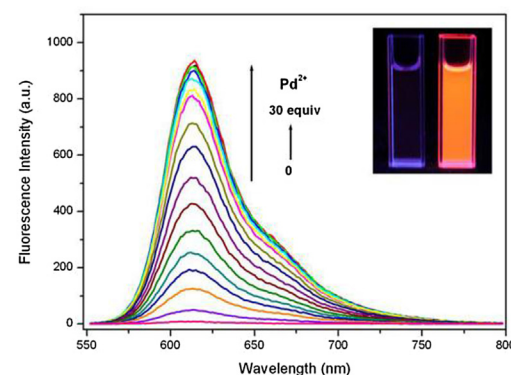


**Fig. 4.** Fluorescence spectra titration of **PDI-1** (5.0  $\mu\text{M}$ ) was measured in the presence of different concentrations of  $\text{Pd}^{2+}$  in  $\text{DMF}/\text{H}_2\text{O}$  (v/v, 7/1) after 30 min,  $\lambda_{\text{ex}}=540$  nm, Slit: 5.0 nm; 5.0 nm. Inset showing the color change (left) before (right) after the addition of  $\text{Pd}^{2+}$  ions in 365 nm light.

palladium (II). More importantly, **PDI-1** also exhibited a similar fluorescence response with other palladium compounds including  $\text{PdCl}_2$ ,  $\text{Pd}(\text{PPh}_3)_2\text{Cl}_2$  (Fig. 5). In the presence of  $\text{Pd}(\text{PPh}_3)_2\text{Cl}_2$  (8.0 equiv), relatively lower but prominent enhancement of fluorescence was observed. That means the counter ions of  $\text{Pd}^{2+}$  does not disturb the sensing process of **PDI-1** towards  $\text{Pd}^{2+}$ .

From the fluorescence titration experimental results (Fig. 6), a good liner relationship between the relative fluorescence

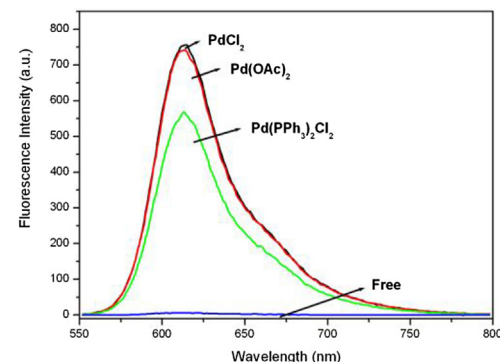


**Fig. 5.** Fluorescence intensity changes of **PDI-1** (5.0  $\mu\text{M}$ ) in the presence of commonly found palladium complexes (8.0 equiv) in  $\text{DMF}/\text{H}_2\text{O}$  (v/v, 7/1),  $\lambda_{\text{ex}}=540$  nm, Slit: 2.5 nm; 5.0 nm.

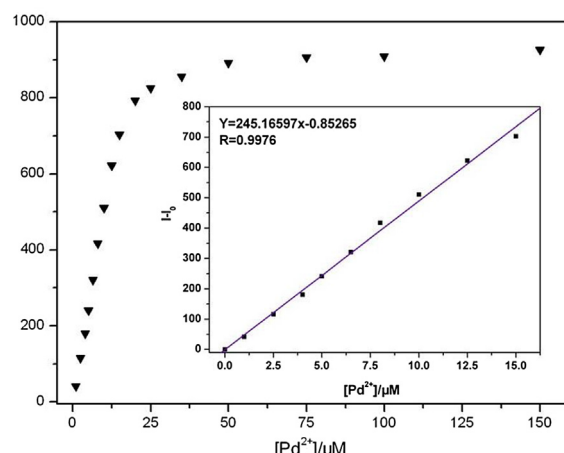


**Fig. 6.** Relative fluorescence intensity of **PDI-1** at different concentrations of  $\text{Pd}^{2+}$  (0–150  $\mu\text{M}$ ) added in  $\text{DMF}/\text{H}_2\text{O}$  (v/v, 7/1). Inset showing a liner relationship between the relative fluorescence intensity and the  $\text{Pd}^{2+}$  concentration.

intensity ( $I - I_0$ ) and the  $\text{Pd}^{2+}$  concentration in the 0–15  $\mu\text{M}$  concentration range ( $R=0.997$ ) was obtained (inset of Fig. 6). This provides a promising method for the quantification of  $\text{Pd}^{2+}$ . By using above-mentioned fluorescence titration results, the detection limit for  $\text{Pd}^{2+}$  was also calculated with the equation: detection limit =  $3\sigma_{\text{bi}}/m$ , where  $\sigma_{\text{bi}}$  is the standard deviation of blank measurements ( $\sigma_{\text{bi}}=0.5984$ , derived from 11 measurements),  $m$  is the slope between relative fluorescence intensity versus sample concentration.<sup>15</sup> The detection limit was measured to be  $7.32 \times 10^{-9} \text{ M}$  (7.32 ppb) in  $\text{DMF}/\text{H}_2\text{O}$  (v/v, 7/1). The detection limit was sufficiently low to detect the nanomolar concentration of  $\text{Pd}^{2+}$ , which means that **PDI-1** can be used for Pd-polluted analysis in drug and environmental settings according to the WHO specified threshold limit for palladium content in drug chemicals [ $4.7 \times 10^{-5} \text{ M}$  (5 ppm) to  $9.4 \times 10^{-5} \text{ M}$  (10 ppm)].<sup>16</sup>

To determine the stoichiometry of the complex between **PDI-1** and  $\text{Pd}^{2+}$ , Job's plot was employed by using the emission intensity as the function of the fraction of  $\text{Pd}^{2+}$ .<sup>17</sup> The result of Job's plot was shown in Fig. S9. The emission intensity reached maximum when the fraction of  $\text{Pd}^{2+}$  was 0.5, indicating a 1:1 stoichiometric complex between **PDI-1** and  $\text{Pd}^{2+}$ , that is, one  $\text{Pd}^{2+}$  ion binds to one molecule of **PDI-1**. In addition, the ESI-MS analysis was conducted to confirm the stoichiometry of the complex between **PDI-1** and  $\text{Pd}^{2+}$  (Fig. S10). A clear peak at  $m/z$  1443.51, corresponding to  $[\text{PDI-1} + \text{Pd}^{2+} + \text{Na}^+ + 2\text{H}^+]$  gave solid evidence for the formation of a 1:1 complex. Based on the 1:1 binding stoichiometry and Benesi–Hildebrand method<sup>18</sup> (Fig. 7, the analysis results could be found in ESI), the plot of  $1/(I - I_0)$  against  $1/[\text{Pd}^{2+}]$  was linear, and the association constant  $K_a$  was calculated to be  $2.24 \times 10^4 \text{ M}^{-1}$ .

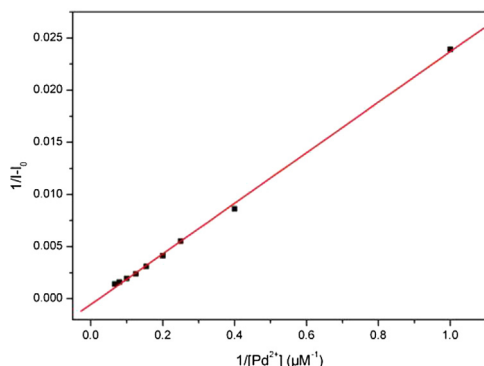


Fig. 7. Benesi–Hildebrand plot of **PDI-1**, assuming 1:1 stoichiometry for association between **PDI-1** and  $\text{Pd}^{2+}$  in  $\text{DMF}/\text{H}_2\text{O}$  (v/v, 7/1).

To get further insight into the binding mode of chemosensor **PDI-1** with  $\text{Pd}^{2+}$ ,  $^1\text{H}$  NMR spectroscopic titration experiment was performed by addition of  $\text{Pd}^{2+}$  to a  $\text{CDCl}_3$  solution of **PDI-1**. The spectral changes are depicted in Fig. 8. Upon addition of 2.0 equiv of  $\text{Pd}^{2+}$ , the  $\text{H}_a$ ,  $\text{H}_b$ ,  $\text{H}_c$ , and  $\text{H}_d$  protons of pyridyl rings underwent overall large downfield shifts of 0.39, 0.20, 0.25, and 0.77 ppm, indicating coordination of nitrogen atoms in pyridyl rings to  $\text{Pd}^{2+}$ . Similarly, the  $\text{H}_f$  and  $\text{H}_g$  aromatic protons of aniline unit experienced downfield shifts of 0.50 and 0.58 ppm, confirming the binding of another nitrogen atom of DPA group to  $\text{Pd}^{2+}$ . In addition, the distinct downfield changes ( $\delta$  4.85 shifting to both 5.39 and 6.17) of chemical shifts ( $\text{H}_e$ ) were also observed. The  $^1\text{H}$  NMR results firmly supported that the nitrogen atoms of the aniline and pyridine rings in DPA moiety were involved in the coordination with  $\text{Pd}^{2+}$ , thus inducing the reduction of PET and the recovery of the fluorescence of PDI. Taking these results into account, a binding mode of  $\text{Pd}^{2+}$  with **PDI-1** was proposed and shown in Fig. 9.

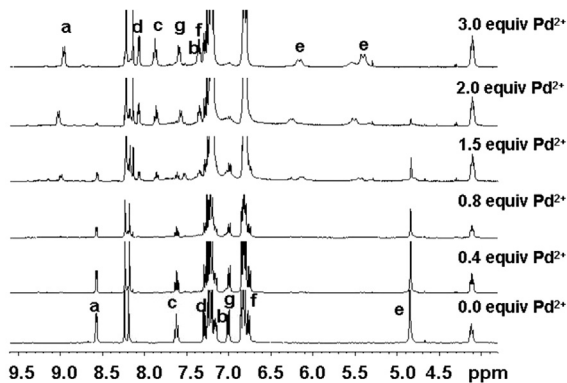


Fig. 8. Partial  $^1\text{H}$  NMR spectra (400 MHz) of **PDI-1** in the presence of different concentrations of  $\text{Pd}^{2+}$  in  $\text{CDCl}_3$ . \*Note: the fluorescence spectra changes of **PDI-1** (5.0  $\mu\text{M}$ ) in the presence of different concentrations of  $\text{Pd}^{2+}$  and job's plot in chloroform were shown in Fig. S12.

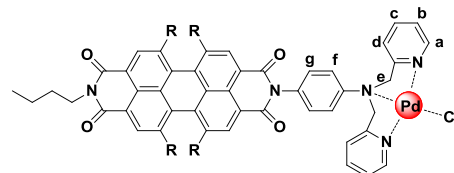


Fig. 9. Proposed binding model of **PDI-1** with  $\text{Pd}^{2+}$ .

The recognition process of **PDI-1** was confirmed to be reversible by adding EDTA to the solution of the metal–ligand complex. The strong fluorescence band at 620 nm was quenched completely after adding excess amount of EDTA (Fig. 10), accompanying with distinctive color change from light pink to dark purple. The dramatic 'on–off' response indicated that EDTA sequestered  $\text{Pd}^{2+}$  from the metal–ligand complex, and regenerated free **PDI-1**. Such reversibility is important for the fabrication of devices to sense the  $\text{Pd}^{2+}$ . Thus **PDI-1** could be classified as a reversible chemosensor for  $\text{Pd}^{2+}$ .

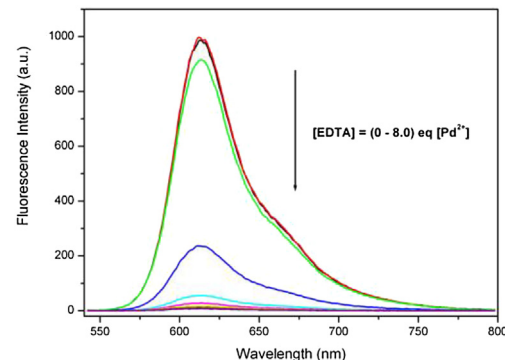
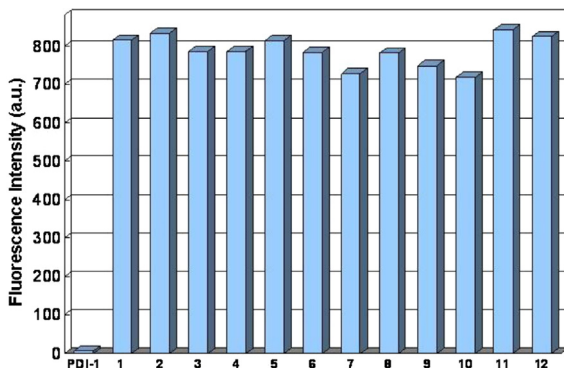


Fig. 10. Fluorescence spectra of **PDI-1** (5.0  $\mu\text{M}$ ) upon gradual addition of  $\text{Pd}^{2+}$  in  $\text{DMF}/\text{H}_2\text{O}$  (v/v, 7/1),  $\lambda_{\text{ex}}=540 \text{ nm}$ , Slit: 2.5 nm; 5.0 nm. EDTA was added to **PDI-1**+ $\text{Pd}^{2+}$  mixture to show the reversible binding nature of  $\text{Pd}^{2+}$  with **PDI-1**.

To further explore the selectivity of **PDI-1** for  $\text{Pd}^{2+}$ , competition experiments were also conducted by recording the fluorescence spectra of **PDI-1** (5.0  $\mu\text{M}$ ) with  $\text{Pd}^{2+}$  in the presence of other competing metal ions under the same concentration (Fig. 11). The fluorescence enhancement observed for the mixtures of  $\text{Pd}^{2+}$  with other metal ions was similar to that caused by  $\text{Pd}^{2+}$  alone. These



**Fig. 11.** Fluorescence responses of **PDI-1** (5.0  $\mu$ M) to  $\text{Pd}^{2+}$  (8.0 equiv) in the presence or absence of other competition metal ions (8.0 equiv). 1= $\text{Pd}^{2+}$  only, 2= $\text{Zn}^{2+}$ + $\text{Pd}^{2+}$ , 3= $\text{Hg}^{2+}$ + $\text{Pd}^{2+}$ , 4= $\text{Fe}^{3+}$ + $\text{Pd}^{2+}$ , 5= $\text{Cr}^{3+}$ + $\text{Pd}^{2+}$ , 6= $\text{Ni}^{2+}$ + $\text{Pd}^{2+}$ , 7= $\text{Ag}^{+}$ + $\text{Pd}^{2+}$ , 8= $\text{Pb}^{2+}$ + $\text{Pd}^{2+}$ , 9= $\text{Co}^{2+}$ + $\text{Pd}^{2+}$ , 10= $\text{Cu}^{2+}$ + $\text{Pd}^{2+}$ , 11= $\text{Mn}^{2+}$ + $\text{Pd}^{2+}$ , 12= $\text{Cd}^{2+}$ + $\text{Pd}^{2+}$ ,  $\lambda_{\text{ex}}=540$  nm, Slit: 2.5 nm; 5.0 nm.

results indicated that other competing metal ions, including  $\text{Ni}^{2+}$ ,  $\text{Cu}^{2+}$ ,  $\text{Zn}^{2+}$ , and  $\text{Cd}^{2+}$ , did not interfere with the binding between **PDI-1** and  $\text{Pd}^{2+}$ , and could not disturb the highly fluorogenic detection of **PDI-1** for  $\text{Pd}^{2+}$  in mixed aqueous solution.

Moreover, the response of **PDI-1** for selective detection of  $\text{Pd}^{2+}$  under different pH conditions was also examined. It was found that the fluorescence intensity of **PDI-1** and **PDI-1** in the presence of  $\text{Pd}^{2+}$  remained stable over a wide pH range of 2.5–10 (Fig. S13). Although the fluorescence intensity of **PDI-1** in a pH range of 0.5–2.5 increased slightly as shown in inset of Fig. S1, but it was negligible in comparison with that induced by  $\text{Pd}^{2+}$ . The results revealed that the fluorescence of the complex formed by **PDI-1** and  $\text{Pd}^{2+}$  was actually pH-independent in the pH range of 2.5–10. **PDI-1** could work as a highly selective and sensitive sensor for  $\text{Pd}^{2+}$  in practical use.

### 3. Conclusion

In summary, three PDI derivatives connecting with DPA moieties using different linkages, **PDI-1**, **PDI-2**, and **PDI-3** were prepared. **PDI-1** showed a remarkable fluorescence enhancement (over 120-fold) in the presence of  $\text{Pd}^{2+}$  in mixed aqueous media with high selectivity over other competing ions, which represented the first example of PET-based ‘turn-on’ probe for  $\text{Pd}^{2+}$ . Moreover, the dramatically ‘off–on’ fluorescence response concomitantly induced the obvious color change from dark purple to brilliant pink, which could also be identified by naked eyes easily. Adding EDTA in the sensing mixture caused significant fluorescence quenching, which indicated that **PDI-1** was a reversible chemosensor. More importantly, the low detection limit was calculated to  $7.32 \times 10^{-9}$  M, which was sufficiently low to detect the nanomolar concentration of  $\text{Pd}^{2+}$ . Hence, **PDI-1** is a highly promising fluorescent chemosensor for the direct quantitative determination of residual  $\text{Pd}^{2+}$  (0–15 ppm) in chemical medicines and environment samples.

### 4. Experimental section

#### 4.1. General methods and materials

NMR spectra were recorded with a 400 MHz spectrometer for  $^1\text{H}$  NMR, 100 MHz for  $^{13}\text{C}$  NMR. Chemical shifts  $\delta$  are given in parts per million (in  $\text{CDCl}_3$ , TMS as internal standard). Absorption spectra were measured on UV-1700 spectrophotometer. Fluorescence emission spectra were measured on a Varian Eclipse FL0905M004 spectrofluorimeter. For column chromatography, silica gel

(200–300 mesh) was used as the stationary phase. All reactions were monitored by thin layer chromatography (TLC).

Compound **1**,<sup>10b,11e,19</sup> compound **2**,<sup>19</sup> compound **3**,<sup>20</sup> and *N-n*-butyl-1,6,7,12-tetra(4-*tert*-butylphenoxy)perylene-3,4:9,10-tetracarboxylic-3,4-anhydride-9,10-imide<sup>21a</sup> were prepared according to literature procedures. The salts used in stock solutions of metal ions were  $\text{Cr}(\text{NO}_3)_3 \cdot 9\text{H}_2\text{O}$ ,  $\text{MnCl}_2 \cdot 4\text{H}_2\text{O}$ ,  $\text{FeCl}_3 \cdot 6\text{H}_2\text{O}$ ,  $\text{CoCl}_2 \cdot 6\text{H}_2\text{O}$ ,  $\text{NiCl}_2 \cdot 6\text{H}_2\text{O}$ ,  $\text{CuCl}_2 \cdot 2\text{H}_2\text{O}$ ,  $\text{Zn}(\text{NO}_3)_2 \cdot 6\text{H}_2\text{O}$ ,  $\text{CdCl}_2 \cdot 2.5\text{H}_2\text{O}$ ,  $\text{AgNO}_3$ ,  $\text{Pd}(\text{OAc})_2$ ,  $\text{Hg}(\text{ClO}_4)_2 \cdot 3\text{H}_2\text{O}$ ,  $\text{Pb}(\text{NO}_3)_2$ . Other chemicals were purchased from commercial sources. Solvents were of chromatographic pure reagent.

### 4.2. Synthesis and characterization

**4.2.1. Synthesis of *N-n*-butyl-*N'*-[*N'',N'''-di(2-pyridylmethyl)-aniline]-1,6,7,12-tetra(4-*tert*-butylphenoxy)perylene-3,4:9,10-tetra carboxylic-3,4:9,10-tetracarboxylic-diimide<sup>21b</sup> (**PDI-1**)***. A solution of compound **1** (90 mg, 0.31 mmol), *N-n*-butyl-1,6,7,12-tetra(4-*tert*-butylphenoxy)perylene-3,4:9,10-tetracarboxylic-3,4-anhydride-9,10-imide (58 mg, 0.056 mmol), and imidazole (500 mg) in toluene (25 ml) was heated to reflux for 12 h under the protection of nitrogen. After cooling, the solvent was removed. The residue was purified by column chromatography on silica gel ( $\text{CH}_3\text{OH}/\text{CH}_2\text{Cl}_2$ , 2/100, v/v) to yield **PDI-1** as violet solid (62 mg, 84%),  $\text{mp}=149\text{--}151$  °C.  $^1\text{H}$  NMR (400 MHz,  $\text{CDCl}_3$ , 25 °C, TMS):  $\delta$  8.58–8.57 (d,  $J=4$  Hz, 2H, pyridine), 8.24 (s, 2H, perylene), 8.19 (s, 2H, perylene), 7.63 (t,  $J=8$  Hz, 2H; pyridine), 7.30–7.29 (d,  $J=4$  Hz, 2H, pyridine), 7.25–7.20 (m, 8H, phenyl), 7.17 (t,  $J=10$  Hz, 2H, pyridine), 7.02–7.00 (d,  $J=8$  Hz, 2H, phenyl), 6.86–6.80 (m, 8H, phenyl), 6.78–6.76 (d,  $J=8$  Hz, 2H, phenyl), 4.85 (s, 4H,  $\text{NCH}_2$ ), 4.12 (t,  $J=8$  Hz, 2H,  $\text{NCH}_2$ ), 1.70–1.63 (m, 2H,  $(\text{CH}_2)_3$ ), 1.45–1.37 (m, 2H,  $(\text{CH}_2)_3$ ), 1.29–1.26 (d,  $J=12$  Hz, 36H,  $\text{C}(\text{CH}_3)_3$ ), 0.94 (t,  $J=8$  Hz, 3H,  $\text{CH}_3$ );  $^{13}\text{C}$  NMR (100 MHz,  $\text{CDCl}_3$ , 25 °C, TMS):  $\delta$  163.4, 163.2, 159.6, 156.0, 153.0, 148.8, 147.3, 136.1, 132.9, 126.7, 122.8, 122.5, 121.8, 120.6, 120.0, 119.5, 119.3, 60.4, 40.4, 38.3, 34.4, 31.5, 30.2, 20.4, 13.8; HR-ESI ( $m/z$ ): calcd for  $\text{C}_{86}\text{H}_{81}\text{N}_5\text{O}_8$ :  $[\text{M}+\text{H}^+]=1312.6085$ , found: 1312.6130.

**4.2.2. Synthesis of *N-n*-butyl-*N'*-( $\text{N''}-2-(\text{N}'',\text{N}'''-\text{di(2-pyridylmethyl)}-\text{amino-ethylene})-\text{aniline}$ )-1,6,7,12-tetra-(4-*tert*-butylphenoxy)-perylene-3,4:9,10-tetracarboxylic-diimide (**PDI-2**)**. A solution of compound **2** (142 mg, 0.37 mmol), *N-n*-butyl-1,6,7,12-tetra(4-*tert*-butylphenoxy)perylene-3,4:9,10-tetracarboxylic-3,4-anhydride-9,10-imide (60 mg, 0.058 mmol), and imidazole (500 mg) in toluene (25 ml) was heated to reflux for 12 h in nitrogen atmosphere. After cooling, the solvent was removed. The residue was purified by column chromatography on silica gel ( $\text{CH}_3\text{OH}/\text{CH}_2\text{Cl}_2$ , 3/100, v/v) to yield **PDI-2** as violet solid (63 mg, 80%),  $\text{mp}=113\text{--}115$  °C.  $^1\text{H}$  NMR (400 MHz,  $\text{CDCl}_3$ , 25 °C, TMS):  $\delta$  8.55–8.54 (d,  $J=4$  Hz, 2H, pyridyl), 8.24–8.23 (d,  $J=4$  Hz, 4H, perylene), 7.62 (t,  $J=8$  Hz, 2H, pyridyl), 7.42–7.40 (d, 2H,  $J=8$  Hz, pyridyl), 7.26–7.21 (m, 8H, phenyl), 7.14 (t,  $J=4$  Hz, 2H, pyridyl), 6.99–6.97 (d,  $J=8$  Hz, 2H, phenyl), 6.83 (t,  $J=10$  Hz, 8H, phenyl), 6.65–6.63 (d,  $J=8$  Hz, 2H, phenyl), 5.02 (br s, 1H,  $\text{NHCH}_2$ ), 4.13 (t,  $J=6$  Hz, 2H,  $\text{NCH}_2$ ), 3.89 (s, 4H,  $\text{NCH}_2$ ), 3.17 (t,  $J=4$  Hz, 2H,  $\text{NCH}_2$ ), 2.88 (t,  $J=4$  Hz, 2H,  $\text{NCH}_2$ ), 1.67–1.65 (m, 2H,  $(\text{CH}_2)_3$ ), 1.45–1.38 (m, 2H,  $(\text{CH}_2)_3$ ), 1.29–1.26 (s, 36H,  $\text{C}(\text{CH}_3)_3$ ), 0.95 (t,  $J=6$  Hz, 3H,  $\text{CH}_3$ );  $^{13}\text{C}$  NMR (100 MHz,  $\text{CDCl}_3$ , 25 °C, TMS):  $\delta$  164.0, 163.5, 159.2, 156.0, 155.9, 152.9, 149.1, 148.7, 147.3, 136.5, 133.0, 128.9, 126.7; 126.6, 123.9, 123.2, 122.8, 122.5, 122.2, 120.6, 120.2, 119.9, 119.8, 119.5, 119.4, 112.9, 67.1, 60.4, 52.8, 41.4, 40.4, 34.4, 31.5, 30.2, 20.4, 13.8. HR-ESI ( $m/z$ ): calcd for  $\text{C}_{88}\text{H}_{86}\text{N}_6\text{O}_8$ :  $[\text{M}+\text{H}^+]=1355.6585$ , found: 1355.6472.

**4.2.3. Synthesis of *N-n*-butyl-*N'*-[ $\text{N}'',\text{N}''-\text{bis(2-pyridylmethyl)}-\text{ethylenediamine}$ ]-1,6,7,12-tetra(4-*tert*-butylphenoxy)perylene-3,4:9,10-tetracarboxylic-3,4:9,10-tetracarboxylic-diimide<sup>22</sup> (**PDI-3**)**. A solution of compound **3** (35 mg, 0.14 mmol) and *N-n*-butyl-1,6,7,12-

tetra(4-*tert*-butylphenoxy) perylene-3,4:9,10-tetracarboxylic-3,4-anhydride-9,10-imide (50 mg, 0.048 mmol) in ethanol was heated to reflux 2 h in nitrogen atmosphere. After cooling, the solvent was removed and the residue was purified by column chromatography on silica gel ( $\text{CH}_3\text{OH}/\text{CH}_2\text{Cl}_2$ , 3/100, v/v) to yield **PDI-3** as violet solid (50 mg, 82%),  $\text{mp}=128\text{--}130^\circ\text{C}$ .  $^1\text{H}$  NMR (400 MHz,  $\text{CDCl}_3$ , 25 °C, TMS):  $\delta$  8.39–8.38 (m, 2H, pyridyl), 8.23 (s, 2H, pyridyl), 8.17 (s, 2H, pyridyl), 7.30–7.31 (m, 4H, perylene), 7.25–7.23 (m, 8H, phenyl), 7.00–6.96 (m, 2H, pyridyl), 6.85–6.82 (m, 8H, phenyl), 4.31 (t,  $J=8$  Hz, 2H,  $\text{NCH}_2$ ), 4.12 (t,  $J=6$  Hz, 2H,  $\text{NCH}_2$ ), 3.85 (s, 4H,  $\text{NCH}_2$ ), 2.88 (t,  $J=8$  Hz, 2H,  $\text{NCH}_2$ ), 1.69–1.62 (m, 2H,  $(\text{CH}_2)_3$ ), 1.42–1.37 (m, 2H,  $(\text{CH}_2)_3$ ), 1.29 (s, 36H,  $\text{C}(\text{CH}_3)_3$ ), 0.93 (t,  $J=8$  Hz, 3H,  $\text{CH}_3$ );  $^{13}\text{C}$  NMR (100 MHz,  $\text{CDCl}_3$ , 25 °C, TMS):  $\delta$  163.4, 163.2, 159.6, 156.0, 155.9, 153.0, 152.9, 148.8, 147.3, 147.3, 136.1, 122.8, 126.7, 122.6, 122.5, 121.8, 120.6, 120.5, 120.0, 119.9, 119.5, 119.3, 119.2, 60.4, 51.8, 40.4, 38.3, 34.4, 31.5, 30.2, 20.4, 13.8; HR-ESI (*m/z*): calcd for  $\text{C}_{82}\text{H}_{81}\text{N}_5\text{O}_8$ :  $[\text{M}+\text{H}^+]=1264.6163$ , found: 1264.6108.

## Acknowledgements

Financial support from the Natural Science Foundation of China (Grant No. 21073112 and 21272059), Science Foundation (2011QK12), and Postdoctoral Science Foundation of Henan Normal University are gratefully acknowledged.

## Supplementary data

Supplementary data ( $^1\text{H}$  NMR and  $^{13}\text{C}$  NMR spectra of **PDI-1**, **PDI-2**, and **PDI-3**, Table S1 and supporting figures (Fig. S7–S13)) associated with this article can be found. Supplementary data related to this article can be found at <http://dx.doi.org/10.1016/j.tet.2014.01.063>.

## References and notes

- (a) De Silva, A. P.; Gunaratne, H. Q. N.; Gunnlaugsson, T.; Huxley, A. J. M.; McCoy, C. P.; Rademacher, J. T.; Rice, T. E. *Chem. Rev.* **1997**, *97*, 1515–1566; (b) Nolan, E. M.; Lippard, S. J. *Chem. Rev.* **2008**, *108*, 3443–3480; (c) Kim, H. N.; Ren, W.; Kim, J. S.; Yoon, J. *Chem. Soc. Rev.* **2012**, *41*, 3210–3244.
- (a) Campiani, G.; Butini, S.; Fattorusso, C.; Trotta, F.; Gemma, S.; Catalano, B.; Nacci, V. *J. Med. Chem.* **2005**, *48*, 1705–1708; (b) Zeni, G.; Larock, R. C. *Chem. Rev.* **2004**, *104*, 2285–2310; (c) Tietze, L. F.; Ila, H.; Bell, H. P. *Chem. Rev.* **2004**, *104*, 3453–3516; (d) Nicolaou, K. C.; Bulger, P. G.; Sarlah, D. *Angew. Chem., Int. Ed.* **2005**, *44*, 4442–4489.
- (a) Kielhorn, J.; Melber, C.; Keller, D. *Environ. Health* **2002**, *205*, 417–432; (b) Spikes, J. D.; Hodgson, C. F. *Biochem. Biophys. Res. Commun.* **1969**, *35*, 420–422; (c) Kawata, Y.; Shiota, M.; Tsutsui, H.; Yoshida, Y.; Sasaki, H.; Kinouchi, Y. *J. Dent. Res.* **1981**, *60*, 1403–1409; (d) Wataha, J. C.; Hanks, C. T. *J. Oral Rehabil.* **1996**, *23*, 309–320; (e) Liu, T. Z.; Lee, S. D.; Bhatnagar, R. S. *Toxicol. Lett.* **1979**, *60*, 469–473; (f) Garrett, C. E.; Prasad, K. *Adv. Synth. Catal.* **2004**, *346*, 889–900.
- (a) Welch, C. J.; Albaneze-Walker, J.; Leonard, W. R.; Biba, M.; Da-Silva, J.; Henderson, D.; Laing, B.; Mathre, D. J.; Spencer, S.; Bu, X.; Wang, T. *Org. Process Res. Dev.* **2005**, *9*, 198–205; (b) Kim, H.; Moon, K.; Shim, S.; Tae, J. *Chem.—Asian J.* **2011**, *6*, 1987–1991.
- (a) Zhou, Y.; Zhang, J.; Zhou, H.; Zhang, Q.; Ma, T.; Niu, J. *Sens. Actuators, B* **2012**, *171*–172, 508–514; (b) Li, H.; Fan, J.; Hu, M.; Cheng, G.; Zhou, D.; Wu, T.; Song, F.; Sun, S.; Duan, C.; Peng, X. *Chem.—Eur. J.* **2012**, *18*, 12242–12250; (c) Li, H.; Fan, J.; Song, F.; Zhu, H.; Du, J.; Sun, S.; Peng, X. *Chem.—Eur. J.* **2010**, *16*, 12349–12356; (d) Goswami, S.; Sen, D.; Das, N. K.; Fun, H.; Quah, C. K. *Chem. Commun.* **2011**, *9101*–9103; (e) Balamurugan, R.; Chien, C. C.; Wu, K. M.; Chiu, Y. H.; Liu, J. H. *Analyst* **2013**, *138*, 1564–1569.
- (a) Zhang, L.; Wang, Y.; Yu, J.; Zhang, G.; Cai, X.; Wu, Y.; Wang, L. *Tetrahedron Lett.* **2013**, *54*, 4019–4022; (b) Wang, C.; Zheng, X.; Huang, R.; Yan, S.; Xie, X.; Tian, T.; Huang, S.; Weng, X.; Zhou, X. *Asian J. Org. Chem.* **2012**, *1*, 259–263; (c) Chen, H.; Lin, W.; Yuan, L. *Org. Biomol. Chem.* **2013**, *11*, 1938–1941; (d) Jiang, J.; Jiang, H.; Liu, W.; Tang, X.; Zhou, X.; Liu, W.; Liu, R. *Org. Lett.* **2011**, *13*, 4922–4925.
- (a) Dissanayake, A. S.; Sandanayake, K. R. A. S. *J. Chem. Soc., Chem. Commun.* **1989**, 1054–1056; (b) Bissell, R. A.; Gunaratne, H. Q. N.; McCoy, C. P.; Sandanayake, K. R. A. S. *Chem. Soc. Rev.* **1992**, *21*, 187–195; (c) Czarnik, A. W. *Acc. Chem. Res.* **1994**, *27*, 302–308; (d) Gunaratne, H. Q. N.; McCoy, C. P. *J. Am. Chem. Soc.* **1997**, *119*, 7891–7892; (e) Prodi, L.; Bolletta, F.; Zaccheroni, N.; Watt, C. I. F.; Mooney, N. *J. Chem.—Eur. J.* **1998**, *4*, 1090–1094; (f) Chen, C. T.; Huang, W. P. *J. Am. Chem. Soc.* **2002**, *124*, 6246–6247; (g) Guo, X.; Qian, X.; Jia, L. *J. Am. Chem. Soc.* **2004**, *126*, 2272–2273; (h) Schwarze, T.; Müller, H.; Holdt, H. J. *Angew. Chem., Int. Ed.* **2007**, *46*, 1671–1674; (i) Kim, J. S.; Quang, D. *T. Chem. Rev.* **2007**, *107*, 3780–3799; (j) Hsieh, W. H.; Wan, C. F.; Liao, D. J.; Wu, A. T. *Tetrahedron Lett.* **2012**, *53*, 5848–5851; (k) Shang, X.; Li, X.; Han, J.; Jia, S.; Zhang, J.; Xu, X. *Inorg. Chem. Commun.* **2012**, *16*, 37–42; (l) Yang, L.; Song, Q.; Cao, H. *Sens. Actuators, B* **2013**, *176*, 181–185; (m) Taki, M.; Akaoka, K.; Iyoshi, S.; Yamamoto, Y. *Inorg. Chem.* **2012**, *51*, 13075–13077; (n) He, G.; Zhao, X. X.; Duan, C. *New J. Chem.* **2010**, *34*, 1055–1058; (o) You, Q. Y.; Wong, R. N. *RSC Adv.* **2012**, *2*, 11078–11083; (p) Sahana, A.; Banerjee, A.; Das, D. *Dalton Trans.* **2013**, *42*, 13311–13314; (q) Liu, X.; Zhang, N.; Zhou, J.; Chang, T.; Fang, C.; Shangguan, D. *Analyst* **2013**, *138*, 901–906.
- (a) Xu, W.; Chen, H.; Wang, Y.; Zhao, C.; Li, X.; Wang, S.; Weng, Y. *Chem.—PhysChem* **2008**, *9*, 1409–1415; (b) Feng, J.; Liang, B.; Wang, D.; Xue, L.; Li, X. *Org. Lett.* **2008**, *10*, 4437–4440.
- (a) Würthner, F. *Chem. Commun.* **2004**, 1564–1579; (b) Wasielewski, M. R. *J. Org. Chem.* **2006**, *71*, 5051–5066; (c) Elemans, J. A. W.; Rowan, A. E. *Adv. Mater.* **2006**, *18*, 1251–1266; (d) Langhals, H. *Helv. Chim. Acta* **2005**, *88*, 1309–1343.
- (a) He, X.; Liu, H.; Li, Y.; Wang, S.; Li, Y.; Wang, N.; Xiao, J.; Xu, X.; Zhu, D. *Adv. Mater.* **2005**, *17*, 2811–2815; (b) Wang, H.; Wang, D.; Wang, Q.; Li, X.; Schalley, C. A. *Org. Biomol. Chem.* **2010**, *8*, 1017–1026; (c) Che, Y.; Yang, X.; Zang, L. *Chem. Commun.* **2008**, 1413–1415.
- (a) Ojida, A.; Sakamoto, T.; Inoue, M.; Fujishima, S.; Lippens, G.; Hamachi, I. *J. Am. Chem. Soc.* **2009**, *131*, 6543–6548; (b) Lee, H. N.; Xu, Z.; Kim, S.; Swamy, K. M. K.; Kim, Y.; Kim, S.; Yoon, J. *J. Am. Chem. Soc.* **2007**, *129*, 3828–3829; (c) Liu, Z.; Zhang, C.; Li, Y.; Wu, Z.; Qian, F.; Yang, X.; He, W.; Gao, X.; Guo, Z. *Org. Lett.* **2009**, *11*, 795–798; (d) Jose, D. A.; Mishra, S.; Ghosh, A.; Shrivastav, A.; Mishra, S. K.; Das, A. *Org. Lett.* **2007**, *9*, 1979–1982; (e) Peng, X.; Du, J.; Fan, J.; Wang, J.; Wu, Y.; Zhao, J. *J. Am. Chem. Soc.* **2007**, *129*, 1500–1501; (f) Ballesteros, E.; Torroba, T. *Org. Lett.* **2009**, *11*, 1269–1272; (g) Bantia, S.; Samanta, A. *New J. Chem.* **2005**, *29*, 1007–1010; (h) Wang, H.; Wu, H.; Xue, L.; Shi, Y.; Li, X. *Org. Biomol. Chem.* **2011**, *9*, 5436–5444; (i) Kwon, J. E.; Nam, W. *Inorg. Chem.* **2012**, *51*, 8760–8774; (j) Zhang, X.; Jing, X.; Liu, T.; Han, G.; Li, H.; Duan, C. *Inorg. Chem.* **2012**, *51*, 2325–2331; (k) Chen, Y.; Jiang, J. *Spectrochim. Acta, Part A* **2013**, *116*, 418–423.
- (a) Chen, Z.; Baumeister, U.; Tschierske, C.; Würthner, F. *Chem.—Eur. J.* **2007**, *13*, 450–465; (b) Würthner, F.; Thalacker, C.; Diele, S.; Tschierske, C. *Chem.—Eur. J.* **2001**, *7*, 2245–2253; (c) Würthner, F.; Thalacker, C.; Sautter, A.; Schärtl, W.; Ibach, W.; Hollricher, O. *Chem.—Eur. J.* **2000**, *6*, 3871–3886; (d) Kaiser, T. E.; Wang, H.; Stepanenko, V.; Würthner, F. *Angew. Chem.* **2007**, *119*, 5637–5640; (e) Jonkheijm, P.; Stutzmann, N.; Chen, Z.; Würthner, F. *J. Am. Chem. Soc.* **2006**, *128*, 9535–9540; (f) Würthner, F.; Chen, Z.; Hoeben, F. J. M.; Osswald, P.; You, C. C.; Jonkheijm, P.; Herrikhuyzen, J. V.; Schenning, A. P. H. J.; Janssen, R. A. J. *J. Am. Chem. Soc.* **2004**, *126*, 10611–10618.
- Zhao, C.; Zhang, Y.; Li, R.; Li, X.; Jiang, J. *J. Org. Chem.* **2007**, *72*, 2402–2410.
- Hazell, A.; Mckenzie, C. J.; Nielsen, L. P. *J. Chem. Soc., Dalton Trans.* **1998**, *11*, 1751–1756.
- Cai, S.; Lu, Y.; He, S.; Wei, F.; Zhao, L.; Zeng, X. *Chem. Commun.* **2013**, 822–824.
- International Programme on Chemical Safety. *Palladium; Environmental Health Criteria Series*; World Health Organization: Geneva, Switzerland, 2002, Vol. 226.
- Vosburgh, W. C.; Cooper, G. R. *J. Am. Chem. Soc.* **1941**, *63*, 437–442.
- (a) Benesi, H. A.; Hildebrand, J. H. *J. Am. Chem. Soc.* **1949**, *71*, 2703–2707; (b) Shiraiishi, Y.; Sumiya, S.; Kohno, Y.; Hirai, T. *J. Org. Chem.* **2008**, *73*, 8571–8574; (c) Würthner, F.; Sautter, A.; Schilling, J. *J. Org. Chem.* **2002**, *67*, 3037–3044.
- Wang, J.; Xiao, Y.; Zhang, Z.; Qian, X.; Yang, Y.; Xu, Q. *J. Mater. Chem.* **2005**, *15*, 2836–2839.
- Hananka, K.; Kikuchi, K.; Urano, Y.; Nagano, T. *J. Chem. Soc., Perkin Trans. 2* **2001**, 1840–1843.
- (a) Feng, J.; Liang, B.; Wang, D.; Wu, H.; Xue, L.; Li, X. *Langmuir* **2008**, *24*, 11209–11215; (b) Feng, J.; Zhang, Y.; Zhao, C.; Li, R.; Xu, W.; Li, X.; Jiang, J. *Chem.—Eur. J.* **2008**, *14*, 7000–7010.
- (a) Bojinov, V. B.; Georgiev, N. I.; Nikolov, P. S. *J. Photochem. Photobiol. A* **2008**, *197*, 281–289; (b) Hu, Y.; Wang, B.; Su, Z. *Polym. Int.* **2008**, *57*, 1343–1350; (c) Xu, Z.; Qian, X.; Zhang, R. *Tetrahedron* **2006**, *62*, 10117–10122.